Removal of antibiotic-resistant bacteria and antibiotic resistance genes affected by varying degrees of fouling on anaerobic microfiltration membranes

Journal:	*Environmental Science & Technology*
Manuscript ID	es-2017-03798u.R1
Manuscript Type:	Article
Date Submitted by the Author:	n/a
Complete List of Authors:	Cheng, Hong; King Abdullah University of Science and Technology Hong, Peiying; King Abdullah University of Science and Technology, Biological and Environmental Science and Engineering

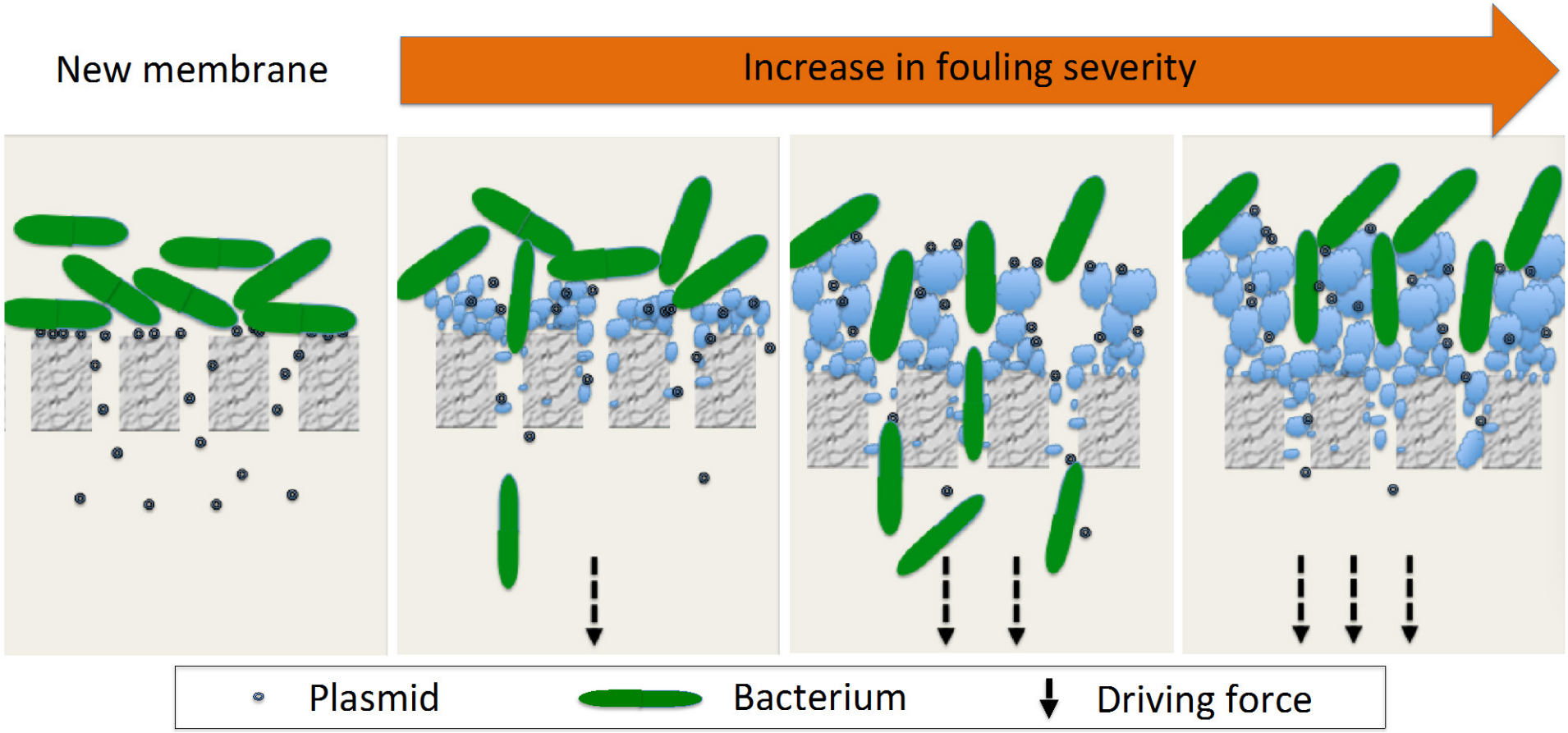
New membrane
Increase in fouling severity
Plasmid
Bacterium
Driving force

Removal of antibiotic-resistant bacteria and antibiotic resistance genes affected by varying degrees of fouling on anaerobic microfiltration membranes

Hong Cheng§, Pei-Ying Hong§*

§King Abdullah University of Science and Technology (KAUST), Division of Biological and Environmental Science & Engineering (BESE), Water Desalination and Reuse Center (WDRC), Thuwal, 23955-6900, Saudi Arabia

*Corresponding author:

Pei-Ying Hong

Email: peiying.hong@kaust.edu.sa

Phone: +966-12-8082218

Keywords: Anaerobic membrane bioreactor, extended-spectrum beta-lactamase, biofouling, transmembrane pressure

Running title: Removal of ARB and ARGs by anaerobic membranes

ABSTRACT

An anaerobic membrane bioreactor was retrofitted with polyvinylidene fluoride (PVDF) microfiltration membrane units, each of which was fouled to a different extent. The membranes with different degrees of fouling were evaluated for their efficiencies in removing three antibiotic-resistant bacteria (ARB), namely, *bla*$_{\text{NDM-1}}$-positive *Escherichia coli* PI-7*, bla*$_{\text{CTX-M-15}}$-positive *Klebsiella pneumoniae* L7 and *bla*$_{\text{OXA-48}}$-positive *Escherichia coli* UPEC-RIY-4, as well as their associated plasmid-borne antibiotic resistance genes (ARGs). The results showed that the log removal values (LRVs) of ARGs correlated positively with the extent of membrane fouling and ranged from 1.9 to 3.9. New membranes with a minimal foulant layer could remove more than 5-log units of ARB. However, as the membranes progressed to subcritical fouling, the LRVs of ARB decreased at increasing operating transmembrane pressures (TMPs). The LRV recovered back to 5 when the membrane was critically fouled, and the achieved LRV remained stable at different operating TMPs. Furthermore, characterization of the surface attributed the removal of both the ARB and ARGs to adsorption, which was facilitated by an increasing hydrophobicity and a decreasing surface zeta potential as the membranes fouled. Our results indicate that both the TMP and the foulant layer synergistically affected ARB removal, but the foulant layer was the main factor that contributed to ARG removal.

1. INTRODUCTION

Municipal wastewater treatment plants have been identified as hotspots for the enrichment of antibiotic-resistant bacteria (ARB) and antibiotic resistance genes (ARGs) and can potentially contribute to the dissemination of ARB and ARGs into the environment [1-3]. In contrast to secondary biological activated sludge processes, which are unable to achieve good removal efficiencies for ARB and ARGs [4, 5], aerobic membrane bioreactors (aeMBRs) were reported in prior studies to achieve > 5.5-log removal of bacteria [6, 7] and > 2.67-log removal of ARGs [8]. However, operating an aeMBR would require high energy consumption rates, and that process produces waste sludge that is viewed as a hotbed for ARB and ARGs [1]. A relatively more sustainable alternative to an aeMBR would be an anaerobic membrane bioreactor (anMBR). An anMBR couples a membrane-based filtration process with anaerobic fermentation, which would not only eliminate the need for aeration but also generate methane as an energy source. Furthermore, anaerobic fermentation has lower sludge production rates compared to activated sludge processes [9].

Despite the advantages of anMBRs compared to aeMBRs, the main drawback for both technologies is membrane biofouling. Biofouling causes a decrease in water flux and higher energy consumption rates and operational costs [10]. Even though several approaches have been developed to alleviate the biofouling of membranes (e.g., backwash, chemical wash, and sonication) [11], the total eradication of the foulant layer is not possible. Therefore, a conventional norm that subcritically fouled membranes remain in operation as long as their flux is not compromised exists. Its existence means that

membranes have an additional foulant layer that has been shown to improve the rejection of bacterial cells and that cleaning the membrane to remove the foulant layer would lead to a reduction of 1 in the log removal values (LRVs) for the bacterial cells in an aeMBR [12]. The mechanism by which fouled membranes retain particles in wastewater results from many factors (e.g., surface characteristics and pore blockage) [13-15]. To illustrate, Cho et al. reported that steric exclusion and aromatic/hydrophobic and charge interactions affect the removal efficiency of natural organic matter [13]. In addition, pore blockage by a cake layer also served to increase the number of retained particles [14, 15].

Earlier studies have reported an approximately 3 to 6-log removal of bacteria in aeMBRs [6, 7, 12]. However, with increased fouling, the transmembrane pressure (TMP) concomitantly rises during the operation, and the operating pressure to drive water through the membrane must increase to maintain a constant flux. Therefore, an increase in the TMP at constant flux may affect the membrane rejection rates. Specifically, this study hypothesizes that an increase in the operating filtration pressure may compromise the LRV for ARB achieved by fouled membranes. This hypothesis has not been systematically assessed in most studies, particularly those that evaluate the performance of anMBRs.

Furthermore, several differences exist between the aerobic and anaerobic foulant layers. To illustrate, Xiong et al. studied the foulant layers attached to membranes connected to aerobic and anaerobic membrane bioreactors of the same reactor configuration [16]. Their findings suggest that when both membrane bioreactors were operated under similar

conditions, differences occurred in the characteristics of both the aerobic and anaerobic foulant layers, specifically in both the concentration and molecular weight of not only the extracellular polymeric substances (EPS) but also the soluble microbial products (SMP). In addition, Yun et al. proved that the anoxic cake layer was more uniform compared to the aerobic one [17]. These differences may mean that the LRVs previously reported for aeMBR systems may not be representative of anMBR systems. As anMBRs are increasingly under consideration for municipal wastewater treatment, differences in their foulant layers compared with those of aeMBRs suggest the existence of a knowledge gap regarding their ability to remove ARB and ARGs.

In the present study, we evaluated the removal efficiency for ARBs and ARGs achieved by anaerobic microfiltration (MF) membranes that were fouled to varying degrees (i.e., N0: new membrane; F1: membrane harvested at ~20 kPa; F2: membrane harvested at ~40 kPa; and F3: membrane harvested at ~60 kPa). Three types of pathogenic ARB (i.e., *E. coli* PI-7, *K. pneumoniae* L7 and *E. coli* UPEC-RIY-4) and their associated plasmid-borne ARGs (i.e., $bla_{\text{NDM-1}}$, $bla_{\text{CTX-M-15}}$ and $bla_{\text{OXA-48}}$) were applied as model contaminants. The genes $bla_{\text{NDM-1}}$, $bla_{\text{CTX-M-15}}$ and $bla_{\text{OXA-48}}$ code for carbapenemases and extended-spectrum beta-lactamases, which are enzymes that confer resistance to carbapenems and other beta-lactam antibiotics. Carbapenems compose a new class of beta-lactam antibiotics that are typically used as a last-resort treatment against gram-negative bacterial infections. The ARB that are resistant as well as the ARGs that confer resistance to such antibiotics are listed as global concerns by the World Health Organization (http://www.who.int/mediacentre/news/releases/2017/bacteria-antibiotics-

needed/en/). These ARB and ARGs were therefore used to determine whether anaerobic membrane bioreactors have the capability of removing these contaminants from wastewaters. Specifically, the aims of this study are to elucidate whether the fouling of anaerobic membranes to varying degrees affects the removal efficiency of biological, emerging contaminants (i.e., ARGs and ARB) and whether the removal rates vary when a fouled membrane is subjected to different operating pressures.

2. MATERIAL AND METHODS

2.1. Reactor configuration and operating conditions. The anMBR operated in this study followed the same configuration (Figure S1A) as that operated in an earlier study [16]. Briefly, the reactor was fed with synthetic wastewater having a chemical oxygen demand (COD) of 750 mg/L and operated at 35 °C and a pH of 7. Two separate runs were conducted (i.e., Run 1 and Run 2), spaced approximately 4 months apart. For each run, three PVDF microfiltration (MF) membranes (GE Osmonics, Minnetonka, MN, USA) that were individually housed in cassette holders were connected in parallel to the anaerobic reactor. The membranes had a nominal pore size of 0.3 μm. The anMBR was operated at a 300 mL/min recirculation rate. Biogas was used to scour the membrane surface at a gas sparging rate of 100 mL/min. The flux was maintained at approximately 7 $L/m^2/h$ (LMH), while the changes in TMP were recorded by a pressure gauge connected to each membrane module (Figure S2). The COD of the effluent was quantified weekly.

143 **2.2. Membrane characterization.** An FEI Nova Nano scanning electron microscope
144 (SEM) was used to characterize a cross section of the cake layer at 5 kV. In preparation
145 for the SEM examination, membrane samples with dimensions of 1 by 2.5 cm were air-
146 dried and then each affixed to an aluminum stub. Iridium was sputtered at a thickness of
147 3 nm onto the membrane surface with a K575X Emitech sputter coater (Quorum
148 Technologies, UK). Atomic force microscopy (AFM) was used to characterize the
149 membrane surface topography. The air-dried membranes were first attached to a support
150 plate and then imaged by an Agilent 5500 AFM system (Agilent Technologies Inc., Palo
151 Alto, CA, USA) in contact mode. Silicon cantilevers (Applied NanoStructures, Inc.; CA;
152 USA) with a resonance frequency of 11–19 kHz and a force constant of 0.1-0.6 Nm^{-1}
153 were used. The acquired AFM images were post-processed by Gwyddion software. For
154 each membrane, five random 10 x 10 μm square pictures were scanned. The contact
155 angle was measured by an EasyDrop shape analyzer (Krüss, Hamburg, Germany) in
156 static mode at ambient temperature to evaluate whether the membranes were hydrophilic
157 ($< 90^{o}$) or hydrophobic ($> 90^{o}$). Ultrapure water was used as the probing liquid, and the
158 mean values were determined from five different independent specimens. The surface
159 zeta potential was measured in a Nano Zetasizer surface cell cuvette containing trace
160 particles (Nano ZS Zen3600, Malvern, UK) at pH 7 and 25 °C, as described elsewhere [18].
161 The membranes to be measured were placed inside the cell cuvette, and the surface zeta
162 potential was evaluated by measuring the zeta potentials of the tracer particles at different
163 distances from the membrane surface. A linear change with distance is observed, and the
164 value at a distance equal to zero is extrapolated automatically by the instrument.
165

2.3. Determination of polysaccharides (PS) and proteins (PN) in soluble extracellular polymeric substances (EPS). The PS and PN concentrations in the soluble EPS fraction from fouled membranes were quantified based on the modified protocols specified by an earlier study [19]. Briefly, the membranes were harvested, placed in 30 mL of sterile 1X M9 minimal salt medium and then vortexed at maximum speed for 2 min to detach the biofilm from the membrane. A 10 mL aliquot of suspension was centrifuged at 10,000 × g for 10 min, and the supernatant was filtered through a 0.22-μm syringe filter (VWR US, Radnor, PA, USA) before its PS and PN contents were determined. The PSs were determined in triplicate for each sample by the phenol-sulfuric acid method. The PNs were quantified in triplicate by a Total Protein Kit (Sigma-Aldrich, St. Louis, MO, USA).

2.4. Filtration experiment for ARB. The MF membranes enclosed in their cassette modules were harvested for the filtration experiments at the TMPs of ~20 kPa, ~40 kPa and ~60 kPa (hereafter named F1, F2 and F3, respectively) (Figure S1B). The membranes harvested at ~20 kPa and ~40 kPa represent subcritically fouled membranes having an increase in the foulant layer corresponding to the TMP level. The membranes harvested at ~60 kPa correspond to critically fouled membranes. The definition for subcritically fouled and critically fouled membranes was made based on the slope of the relationship between the TMP profile and the duration (Figure S2). The subcritically fouled membranes were defined as those with a TMP that increased at an exponential rate to maintain a constant flux (ca. 7 LMH). The critically fouled membranes were defined as those with TMP that reached a plateau and were no longer capable of further increases to

maintain a constant flux. Three types of ARB, namely, *bla*$_{NDM-1}$-positive *E. coli* PI-7 [20] marked with green fluorescence protein, *bla*$_{CTX-M-15}$-positive *K. pneumoniae* L7 [21] and *bla*$_{OXA-48}$-positive *E. coli* UPEC-RIY-4 were spiked into sterile 1X M9 minimal salt medium (Sigma-Aldrich, St. Louis, MO, USA) to obtain a final OD_{600} of ~0.3. The growth conditions for each ARB are provided in Supplementary Material S1. The culture suspension with bacteria was independently filtered through the F1, F2 and F3 membranes. The same culture suspensions were also filtered through new membranes. All the filtration experiments were operated at a recirculation rate of 300 mL/min and a nitrogen sparging rate of 100 mL/min to approximate the same conditions experienced in the anMBR.

During the filtration experiment, the filtration TMP was incrementally adjusted for F1, F2 and F3 to determine whether an increase in filtration pressure would affect the removal efficiencies achieved by each type of fouled membrane. The permeate was sampled every 4 h prior to increasing the filtration TMP. For example, the filtration TMP for F1 was incrementally increased from 5 kPa to 10 kPa, then to 15 kPa and finally to 20 kPa (the permeates collected at each TMP are hereafter referred to as F1-1, F1-2, F1-3 and F1-4, respectively). Similarly, for F2, the TMP was incrementally adjusted from 10 kPa to 20 kPa, 30 kPa and finally 40 kPa (the permeates collected at each TMP are hereafter referred as F2-1, F2-2, F2-3 and F2-4, respectively). For F3, the filtration TMP was increased from 10 kPa to 20 kPa, 40 kPa and 60 kPa sequentially (the permeates collected at each TMP are hereafter referred as F3-1, F3-2, F3-3 and F3-4, respectively) (Table S1). The filtration experiment with the new membrane was performed at fluxes matching those of the F1 membranes. In all instances, no filtration TMP was observed with the new

membrane since no foulant layer existed. The permeate was collected at the same abovementioned intervals to provide corresponding controls, and these permeates are hereafter referred as N0-1, N0-2, N0-3 and N0-4, respectively. Table S1 summarizes the matrix of conditions used in this study. At the end of the filtration experiments, all the membranes were harvested for characterization, as detailed in section 2.3. The biofilm attached to the membranes and the permeate were processed and extracted for their total DNA, as previously described [19].

2.5. Filtration experiment for ARGs. A 60 mL sample of each bacterial host was incubated in a 200 rpm shaker incubator for 17 h at 37 °C and then extracted for its plasmids by the PureYield^{TM} Plasmid Miniprep System (Promega, Madison, WI, USA). Earlier work sequenced the *bla*$_{NDM-1}$-positive plasmid [3], and the associated plasmid size was known. In addition, the present study sequenced the *bla*$_{CTX-M-15}$-positive plasmid associated with *K. pneumoniae* L7 and the *bla*$_{OXA-48}$-positive plasmid associated with *E. coli* UPEC-RIY-4 via the Illumina MiSeq platform (Illumina, San Diego, CA, USA). The specific protocols detailing the sequencing and assembly are provided in Supplementary Material S2. The plasmids were spiked into sterile 1X M9 minimal salt medium to a final concentration of ~10^5 copies/mL. The filtration experiment for the ARGs was conducted in a manner similar to that described in section 2.4 but without the increments in the filtration TMP. After the filtration experiment, the membranes were harvested for characterization, as detailed in section 2.3. Six milliliters of each biomass suspension and permeate were frozen at -80 °C and lyophilized using a Christ Alpha 1-2 LDplus freeze

234 dryer. The lyophilized biomass suspension and permeate were subjected to DNA
235 extraction, as previously described [22].
236
237 **2.6. Quantification of ARB and ARGs.** The ARB were quantified by determining their
238 associated ARG marker. The quantification of the associated ARGs (i.e., $bla_{\text{NDM-1}}$,
239 $bla_{\text{CTX-M-15}}$ and $bla_{\text{OXA-48}}$) was conducted with an Applied Biosystems 7900HT Fast Real-
240 Time PCR (qPCR) System (Thermo Fisher Scientific, Carlsbad, CA, USA). The TaqMan
241 probes and corresponding primer sequences are listed in Table S2. The qPCR standards
242 for the associated genes were prepared as described previously [23]. The thermal cycle and
243 detection limit are shown in Supplementary Material S3. In addition, to verify the qPCR
244 result, flow cytometry by the BD FACSCanto II system ((BD Biosciences, San Jose, CA,
245 USA) was used to determine the cell counts of the $bla_{\text{NDM-1}}$-positive *E. coli* PI-7, based
246 on the green fluorescence protein.
247
248 **2.7. ARB adsorption comparison.** To compare adsorption between the ARB and the
249 foulant layer, isothermal titration calorimetry (ITC) was applied (Malvern ITC200,
250 Malvern, UK). ITC measures the heat change that occurs when two substances interact. *E.*
251 *coli* PI-7, *K. pneumoniae* L7 and *E. coli* UPEC-RIY-4 were respectively incubated in a
252 200 rpm shaker incubator for 17 h at 37 °C and then centrifuged at 10,000 g for 10 min to
253 obtain cell pellets. The cell pellets were resuspended and washed twice with M9 minimal
254 salt medium and recentrifuged before the washed pellets were finally resuspended in M9
255 minimal salt medium and diluted to a final OD_{600} of 0.3. Ten milliliters of the different
256 foulant suspensions from section 2.3 was filtered through 40 μm Falcon™ Cell Strainers

(Fisher Scientific, USA). The filtrate was respectively aliquoted and then diluted 1:4 v/v in M9 minimal salt medium. Two microliters of the filtrate was injected into 200 µL of each ARB suspension at 25 °C using a 750 rpm stirring speed and 4 s duration. Each sample was injected into the ITC machine a total of 12 times, with a 120 s interval between each injection. The resulting values were analyzed and plotted using Origin (version 7).

2.8. Statistical analysis. Significance was analyzed either by a two-tailed t-test, available in Microsoft Excel 2013, or by one-way ANOVA, available in Minitab Express.

3. RESULTS

3.1. Differences in the thickness and the PS and PN concentrations of F1, F2 and F3 membranes. As fouling progressed from F1 to F3, the thickness of the foulant layer, as evidenced from the cross-sectional images of the membranes, revealed a corresponding increase (Figure S3). Its thickness for F1 was approximately 2.99 ± 0.17 µm in Run 1 and 3.96 ± 0.26 µm in Run 2 (Table 1). When the TMP increased to ~40 kPa (i.e., F2), the foulant layer thickness increased by > 2 times compared to that for F1 (8.80 ± 0.13 µm in Run 1 and 10.43 ± 0.48 µm in Run 2). F3, the critically fouled membrane, had a foulant layer thickness of 26.92 ± 3.24 µm in Run 1 and 20.33 ± 0.43 µm in Run 2. The estimated biovolume increased from F1 to F3 with the increasing thickness (Table 1). The polysaccharide (PS) concentration increased significantly as fouling progressed (t-test, $p < 0.01$), rising from 17.53 and 25.63 µg/cm^2 in Run 1 and Run 2, respectively, for

F1 to 73.89 and 45.18 μg/cm^2 in Run 1 and Run 2 for F2. For F3, the PS concentration further increased to 96.56 and 133.27 μg/cm^2 in Run 1 and Run 2, respectively (Figures S4A and S4C). Similarly, the protein (PN) concentration also increased significantly from F1 to F3 (t-test, $p < 0.01$). The PN concentration in the foulant layer was 4.36 and 5.00 μg/cm^2 in Run 1 and Run 2, respectively, for F1. These values increased for F3 to 19.36 and 25.50 μg/cm^2 in Run 1 and Run 2, respectively (Figures S4B and S4D).

3.2. Differences in the surface characteristics of F1, F2 and F3 membranes. Among all the tested membranes, the new membrane (i.e., N0) had the roughest surface area (R_a = 118.3 ± 27.0) and was significantly rougher than the three fouled membranes (i.e., F1, F2 and F3) (t-test, $p < 0.01$) (Table 1). As the membranes fouled, the hydrophobicity of the membrane surfaces increased (Table 1). The new PVDF membrane was hydrophilic (78.7 ± 3.8°), but the presence of a foulant layer caused the contact angle to increase to 90.2 ± 2.3° for F1, indicating that the membrane surface became hydrophobic. The contact angle further increased to 95.5 ± 2.3° and 107.4 ± 1.6° for F2 and F3, respectively. In addition, the new membrane exhibited the lowest surface zeta potential (i.e., -44.3 ± 4.4 mV) (Table 1). In contrast, the surface zeta potential values for the fouled membranes were -17.3 ± 0.3 mV, -19.2 ± 1.9 mV and -25.8 ± 2.3 mV; these membranes showed a significantly lower negative charge than that measured for the new membrane (t-test, $p < 0.01$).

3.3. ARGs showed smaller particulate sizes but a higher negative charge compared to ARB. The results obtained from the dynamic light scattering technique indicated that

303 the average particulate size of *E. coli* PI-7, *K. pneumoniae* L7 and *E. coli* UPEC-RIY-4
304 was 1899.4 ± 235.4 nm, 1956.2 ± 253.0 nm, and 2141 ± 33.9 nm, respectively. In
305 contrast, all of the three plasmids were smaller than 565 nm (Figure S5A). The zeta
306 potential assessments of plasmids showed that all three plasmids and the ARBs were
307 negatively charged. The absolute zeta potential value of plasmids was greater than 22
308 mV; in contrast, the absolute charge of bacteria was always less than 15 mV (Figure
309 S5B).
310
311 **3.4. Increase in LRV for ARGs with fouling severity.** In Run 1, the new membrane
312 achieved an LRV of 2.75 for the plasmid encoding the $bla_{\text{NDM-1}}$ gene. The LRVs achieved
313 by F1, F2 and F3 were higher, reaching 3.48, 3.60 and 3.84, respectively (Figure 1A). A
314 similar increment in the LRV was observed for the plasmid encoding the $bla_{\text{OXA-48}}$ gene.
315 To illustrate, the LRV achieved by the new membrane was 1.90, but this value increased
316 to 3.37 for F2. No $bla_{\text{OXA-48}}$-encoding plasmid was detected in the F1 or F3 permeates.
317 Likewise, no $bla_{\text{CTX-M-15}}$-encoding plasmid was detected in any of the permeate samples,
318 and no LRVs could be obtained.
319 To confirm that the LRVs of the ARG-encoding plasmids were higher in the presence of
320 fouled membranes, a replicate run was conducted. In Run 2, the LRVs achieved by new
321 membrane were 2.30, 2.13 and 2.42 for the plasmids encoding $bla_{\text{NDM-1}}$, $bla_{\text{CTX-M-15}}$ and
322 $bla_{\text{OXA-48}}$, respectively (Figure 1C). In contrast, all the LRVs for the fouled membrane
323 were higher than 2.76, and the LRV increased as fouling progressed. The LRV of the
324 plasmid encoding $bla_{\text{NDM-1}}$ achieved by F1, F2 and F3 were 1.3-, 1.2- and 1.5-fold higher
325 than that achieved by the new membrane. Similarly, the LRV for the plasmid encoding

326 $bla_{\text{CTX-M-15}}$ increased to 3.35 and 3.45 on the F1 and F2 fouled membranes, and no
327 detectable $bla_{\text{CTX-M-15}}$ was present in the F3 permeate. In addition, the LRVs for the
328 plasmid encoding $bla_{\text{OXA-48}}$ were higher using the fouled membranes compared to the
329 new membrane (Figure 1C).
330
331 **3.5. Foulant layer enhanced the adsorption of ARGs.** The abundance of plasmids
332 encoding the $bla_{\text{NDM-1}}$ gene and attached to the new membrane was approximately 1.90 x
333 10^3 and 5.51 x 10^2 copies/cm^2 in Run 1 and Run 2, respectively. In contrast, the respective
334 abundance of these plasmids attached to the F1, F2 and F3 membranes increased to 2.61
335 x 10^5, 1.46 x 10^4 and 3.11 x 10^4 copies/cm^2 for Run 1; and these abundances were
336 significantly higher than that obtained for this plasmid using the new membrane (t-test, $p < 0.01$) (Figure 1B). In Run 2, the abundances of the plasmid encoding $bla_{\text{NDM-1}}$ and
338 attached to the fouled membranes were up to 74 times higher than the abundance of this
339 plasmid detected on the new membrane (Figure 1D). Similar trends were observed for the
340 other two plasmids (Figures 1B and 1D).
341
342 **3.6. New membrane and critically fouled F3 membrane displayed high LRVs for**
343 **ARBs.** The qPCR results indicated that new membrane can achieve a high LRV for all
344 the tested ARB. To illustrate, the average LRVs were 6.50, 6.50 and 5.39 in Run 1 for *E.*
345 *coli* PI-7, *K. pneumoniae* and *E. coli* UPEC-RIY-4, respectively. The same range of
346 LRVs was achieved in Run 2 (Figures 2A to 2C). In contrast, the average LRV achieved
347 by F1 for *E. coli* PI-7 decreased to 3.48 and 4.99. The average LRV further decreased to
348 1.28 and 2.18 in the two runs for *E. coli* PI-7 when a more heavily fouled F2 membrane

was tested. However, the average LRV for the F3 treatment increased in both runs to approximately that achieved by the new membranes (Figure 2A), and the LRVs obtained for F3 and for the new membranes were not significantly different (one-way ANOVA, $p > 0.05$). Specifically, the LRV for *E. coli* PI-7 was 5.19 in Run 1 and 4.51 in Run 2. These LRVs achieved by F3 were, however, significantly higher than those achieved by F2 (one-way ANOVA, $p < 0.01$). The same trend was also observed for the average LRVs of *K. pneumoniae* and *E. coli* UPEC-RIY-4 as the severity of membrane fouling progressed (Figures 2B and 2C).

A further evaluation was undertaken to determine whether an increase in the filtration pressure would affect the LRV achieved by membranes fouled to different degrees. For the F1 and F2 subcritically fouled membranes, an increase in filtration pressure resulted in a decreased LRV in most instances. For example, with the exception of the LRVs achieved for all the ARB by the F1 membrane in Run 2, both runs showed that the subcritically fouled F2 membranes experienced up to 2-log declines in the LRVs for all three ARB groups when the filtration pressure was increased (Figures 2A to 2C). In both runs, the LRVs achieved by the F2 membranes at the higher filtration pressures (i.e., F2-3 and F2-4) were significantly less than the LRVs achieved at the lower filtration pressures (i.e., F2-1 and F2-2) (one-way ANOVA, $p < 0.05$).

In contrast to the subcritically fouled membranes, increasing the filtration pressure applied to the critically fouled F3 membrane did not significantly affect the average LRV of any tested ARB (one-way ANOVA, $p > 0.59$).

371 **3.7. Foulant layer enhanced the attachment of ARB.** The abundance for *E. coli* PI-7
372 attached per cm^2 of the new membrane was 4.92 x 10^6 in Run 1, which was significantly
373 lower than that of the F1, F2 and F3 membranes (t-test, $p < 0.05$) (Figure 3A). In Run 2,
374 the abundance of *E. coli* PI-7 attached per cm^2 of the F1, F2 and F3 membranes was 2.41
375 x 10^7, 2.40 x 10^7, and 4.25 x 10^7, respectively, and these abundances were significantly
376 higher than that on the new membrane by as much as 1-log unit (t-test, $p = 0.01$) (Figure
377 3B). Similarly, the abundance of *K. pneumoniae* L7 and *E. coli* UPEC-RIY-4 attached to
378 the new membrane was significantly lower than that on the F1, F2 and F3 membranes in
379 both runs (t-test, $p < 0.05$) (Figures 3A and 3B).
380 The interaction between the ARB and the foulant layer was confirmed by ITC (Figure 4).
381 Compared to the blank which did not contain any foulant, the presence of foulant
382 obtained from F1, F2 and F3 membranes released significantly more heat upon
383 interaction with the three ARB (t-test, $p < 0.01$). In addition, the heat release was highest
384 when foulant layer obtained from F3 was present. To illustrate, the heat change for F1
385 was 0.035 μcal/s upon interaction with *E. coli* PI-7, and this value increased by 46.9%
386 and 59.9% for F2 and F3, respectively, compared to that for F1.
387
388 **3.8. Experiment to verify the LRV for *E. coli* PI-7.** To verify the result obtained by
389 qPCR, flow cytometry was applied as an alternative method to assess the LRV and the
390 abundance of the *E. coli* PI-7 cells adhered to the membrane surfaces (Figure S6). To
391 illustrate, the average, *E. coli* PI-7 LRV for the new membrane was 5.95 in Run 1 and
392 5.19 in Run 2. For F1, the LRV decreased to 2.89 in Run 1 and 3.35 in Run 2. However,
393 the LRV recovered to 3.92 in Run 1 and 4.27 in Run 2 for F3. A further evaluation

394 regarding the abundance of *E. coli* PI-7 attached to the membrane surfaces revealed
395 higher cell counts on the fouled than on the new membranes (Figure S7). The
396 number/cm^2 of *E. coli* PI-7 attached to the new membrane was 6.64 x 10^4 in Run 1 and
397 1.40 x 10^5 in Run 2. In contrast, the abundance of *E. coli* PI-7, measured as the number of
398 bacteria attached per cm^2 of fouled membrane (i.e., F1, F2 and F3), ranged from 2.37 x
399 10^6 to 1.57 x 10^7 in Run 1 and from 3.62 x 10^6 to 3.20 x 10^7 in Run 2.
400
401
402 **4. DISCUSSION**
403 The World Health Organization has warned in their 2014 Global Report on Surveillance
404 that "antimicrobial resistance threatens the effective prevention and treatment of an ever-
405 increasing range of infections caused by bacteria, parasites, viruses and fungi" [24].
406 Because of the widespread use of antibiotics, resistant organisms, including their mobile
407 genetic elements, exist almost ubiquitously in humans, animals, food and the
408 environment. In particular, wastewater has been identified as an important reservoir that
409 can disseminate such resistant organisms and mobile genetic elements into the
410 environment or to end users during reuse events [1, 25]. These concerns may impede
411 subsequent effort to reuse treated wastewaters.
412
413 As such, an effective treatment process is needed to remove ARB and ARGs from
414 wastewater prior to its discharge or reuse. An earlier study assessed the LRVs for these
415 emerging contaminants (i.e., ARB and ARGs) achieved by full-scale aerobic MBRs and
416 determined that the concentrations of ARGs (e.g., tetW, tetO, and sulI) and ARB (e.g.,

417 tetracycline- and sulfonamide-resistant bacteria) in the post-MBR permeate stream were
418 1 to 3-log units less than those achieved by activated sludge processes [8], suggesting that
419 membrane systems are more effective than the conventional activated sludge in removing
420 these emerging contaminants from wastewater. Studies have also been conducted to
421 assess the LRVs for contaminants (e.g., organic micropollutants, bacterial pathogens, and
422 viruses) achieved by anMBRs [26-28], which in recent years, are proposed as a sustainable
423 alternative to aerobic MBRs for municipal wastewater treatment. For instance, Wei et al.
424 investigated the removal of 15 organic micropollutants by a laboratory-scale anMBR and
425 found 80–92% rejection rates for most organic micropollutants [26]. Harb et al. further
426 reported that a laboratory-scale anMBR can achieve > 1.7-log removal of opportunistic
427 pathogenic species from municipal wastewater [27]. In addition, Wong et al. reported a 3.7
428 log removal of coliphages by an anMBR [28].
429
430 Nevertheless, most of these existing studies do not evaluate for the removal efficiencies
431 of ARBs and ARGs by anMBRs. In the present study, the LRVs of three plasmids
432 encoding for ARGs ranged from 2.76 to 3.84-log units when the anaerobic membrane
433 became increasingly fouled (Figures 1A and 1C). These reported LRVs approximately
434 match the LRV obtained by Wong and coworkers for viruses [28]. This similarity occurred
435 despite differences between the viruses and plasmids evaluated in the two studies.
436 Viruses such as adenovirus, enterovirus and coliphage have genome sizes that range from
437 3600 nt to 48 kbp, depending on whether the virus is a single-stranded RNA virus or a
438 double-stranded DNA virus. These genome sizes would equate to an approximate viral
439 particle diameter of 30 to 100 nm. In comparison, these sizes are much smaller than those

of the plasmids that were evaluated in the present study. The plasmid sequencing did not result in a complete assembly of the plasmids that encode for $bla_{\text{CTX-M-15}}$ and $bla_{\text{OXA-48}}$. However, the assembled contigs of the partial plasmidic genomes have already revealed a size as large as 110 kbp and 55 kbp for these two plasmids (i.e., $bla_{\text{CTX-M-15}}$ and $bla_{\text{OXA-48}}$) [21]. Similarly, the IncF plasmid encoding for $bla_{\text{NDM-1}}$ is reported to have a size as large as 110 kbp [3]. Collectively, the plasmids assessed in the current study show comparatively larger genome sizes and are thus likely to have larger particulate sizes compared to viruses. To verify this supposition, the particulate size of all three plasmids used in the current study were further assessed by a dynamic light scattering technique and were found to be ca. 460 to 560 nm in diameter (Figure S5A).

Furthermore, viruses have capsid proteins that are hydrophobic [29], while extracellular plasmids are generally hydrophilic due to the exposed sugar-phosphate bond of DNA [30]. In the present study, significantly more plasmids were found attached to the fouled compared to the new membranes. This pattern occurred despite no clear correlation between the attachment preference and the surface characteristics. For example, hydrophobicity increases as anaerobic membranes become progressively fouled, and both the membrane surface and the plasmids showed a negative charge (Table 1 and Figure S5B). These conditions would have led to hydrophobic-hydrophilic and charge repulsion between the membrane surfaces and plasmids. However, the abundance of the plasmids that attached to the membranes remained within the same range (Figures 1B and 1D). This effect may have been due to the presence of an electrolyte in the M9 minimal salt medium used during the filtration experiment, which led to a decrease in the repulsion

463 force exhibited in hydrophobic-hydrophilic and charge interactions [31]. In addition, new
464 membrane exhibits a rougher surface area compared to fouled membranes, which is
465 generally thought to facilitate adhesion [32, 33]. Instead, a significantly lower abundance of
466 attached plasmids occurred on the new membranes compared to the fouled ones with
467 relatively smooth surfaces (Figures 1B and 1D).
468
469 Despite a lack of understanding regarding the exact mechanisms governing the
470 attachment of plasmids to anaerobic membranes, the presence of foulant improved the
471 removal efficiency for all three of the plasmids. However, the LRVs achieved by
472 membranes fouled to different degrees (i.e., F1, F2, and F3) were similar. This pattern
473 occurred despite an increase in the thickness of the foulant layer (Table 1), suggesting
474 that size exclusion and biovolume are less important factors than adsorption in removing
475 plasmids (Figures 1B and 1D). A higher adsorption of plasmids on the fouled membranes
476 compared to the new membrane was likely due to the higher protein and polysaccharide
477 concentrations measured in the foulant layer of the fouled membranes, which facilitated
478 interaction and the adsorption of the plasmids to the foulant layer. In addition, the
479 presence of a cake layer on the fouled membranes would induce a more severe
480 concentration polarization [37] than that experienced on the new membrane. Previous
481 studies have shown that concentration polarization improves the rejection of volatile
482 organic compounds, perfluorooctane sulfonates, boron and arsenic [34-36]. Similarly,
483 concentration polarization may have also contributed to the high LRVs for the ARGs
484 achieved by the fouled membranes evaluated in the current study.
485

Apart from ARG filtration, the current study also investigated the LRVs for three ARB. Prior studies have determined that both *E. coli* and *K. pneumoniae* possess a hydrophobic cell surface [38, 39], which would facilitate bacterial attachment to the hydrophobic anaerobic membranes (Figure 3). In addition, the relatively lower negative charge of bacteria compared to plasmids would have resulted in less charge repulsion and thus adsorption onto the membranes (Figure S5B). Although the number of cells attached to the three fouled membranes was significantly higher compared to the new membrane, no significant difference existed among the number of cells attached to the three fouled membranes. This observation implies that other factors (e.g., extracellular polymeric substances, cake layer thickness) and not solely surface properties affect the adhesion of ARB to fouled membranes. To verify this supposition, ITC was used as an alternative method to detect and compare the interaction between the ARB and the foulant layers. Unlike the traditional atomic force microscope (AFM) method, which modifies the AFM tips to detect the interaction force [40, 41], the ITC method measures the heat change that occurs when two molecules interact [42], which is directly proportional to the level of interaction. When compared to the heat change obtained from the interaction between the bacterial suspensions and the control (i.e., M9 minimal salt medium with no biofilm suspension), more heat was released when the biofilm suspensions obtained from the fouled membranes were injected into the bacterial suspensions (Figure 4). This observation indicates that the ARB can interact with the biofilm matrix, hence accounting for the higher attachment of cells onto the fouled membranes compared to the new one.

508 The present study further aims to determine whether different filtration pressures applied
509 to these fouled membranes affect their ARB removal efficiencies. The results suggest that
510 when anaerobic membranes are subcritically fouled and the filtration pressure is
511 increased, the removal of ARB is compromised. However, a lower LRV was not
512 observed when the membranes were critically fouled, despite a subsequent increase in
513 filtration pressure.
514
515 The ARB used in this study were found to be of ca. 2000 nm in particulate size (Figure
516 S5A and Figure S8). Antimicrobial molecules are known for inducing alterations in the
517 bacterial envelope and in its mechanical properties, such as the cell wall elasticity [43, 44].
518 Prior study indicates that the cell wall is an important factor in triggering the passage of
519 bacteria through membranes with a relatively small pore size [45-47]. An earlier study found
520 that antibiotics present in the suspension medium affect the mechanical properties of the
521 bacterial cell wall by decreasing its rigidity, thereby resulting in a greater number of cells
522 passing through a membrane and entering into the permeate stream. However, whether
523 ARB have a higher deformability compared to antibiotic-susceptible bacteria is unknown.
524 Gram-negative bacteria were also demonstrated to cross through membrane barriers by
525 deforming themselves under high filtration pressures of 10 to 950 kPa [48, 49]. Earlier study
526 has also shown that the particle size in the cake layer from anaerobic membranes
527 decreases from the top to the bottom layer, resulting in a corresponding decrease in
528 porosity across the different layers [50, 51]. This gradual decrease in pore size formed
529 funnel-like structures that would likely facilitate the passage of less rigid cells through
530 membrane pores. Coupled with findings suggesting that an increase in transmembrane

pressure could enlarge membrane pore size [52], these factors can possibly explain why subcritical fouling would lower the LRV for ARB when the filtration pressure increases.

However, the LRVs achieved by the critically fouled membranes returned to a lower level approximating that achieved by the new membranes (Figure 2). This result could be explained by the total blockage of membrane pores via an irremovable foulant layer at that fouling level; therefore, any further increase in the filtration pressure was unable to force deformed cells through the membrane barrier. A total pore blockage is facilitated by the high protein concentration measured in the biofilm matrix of the anaerobic membrane in this study (Figures S4B and S4D) and in an earlier study [16]. These high protein contents may, in turn, contribute significantly to the blockage of anaerobic membrane pores [53, 54].

In summary, the findings from the present study suggest that as anaerobic membranes fouled progressively, the total LRV for the ARGs increased while that for the ARB initially decreased before subsequently stabilizing at an LRV similar to that of new microfiltration membranes. In particular, for subcritically fouled membranes, a lower LRV for the ARB was attained with an increase in filtration pressure. However, the same compromise in the LRVs was not observed when the membranes were critically fouled. These results collectively suggest that an MBR shows promise in removing at least 2 to 3-log units of ARB and ARGs, especially when operated in the long term to favor high removal rates of both ARB and ARGs.

554 **5. Acknowledgments**

555 The authors would like to thank Mr. Qingtian Guan for providing technical assistance
556 with plasmid assemblies. This study is supported by KAUST Center Competitive
557 Funding FCC/1/1971-06-01 awarded to P.-Y. Hong.

558

559 **Supplementary Information Available**

560 Methods: Growth conditions for antibiotic-resistant bacteria; Plasmid sequencing and
561 assembly; Real-time PCR and detection limit test; Analysis of particulate sizes; Zeta
562 potential analysis.
563 Tables: Matrix of conditions used in this study; Primers and fluorogenic probes for the
564 specific detection of resistance genes.
565 Figures: Schematic diagram of anaerobic membrane reactors and experimental setup for
566 the ARB and ARG filtration experiment; Changes in transmembrane pressure for the
567 different microfiltration membranes; Cross-sectional SEM images of membranes;
568 Concentration of polysaccharides and proteins in soluble EPS; Particulate size and zeta
569 potential of ARB and ARGs; LRV of *E. coli* PI-7 assessed by flow cytometry;
570 Abundance of *E. coli* PI-7 attached to membranes assessed by flow cytometry; SEM
571 images of ARB.

572 **Table 1** Roughness, hydrophilicity and surface zeta potential of different membranes. N.A. denotes not applicable.

Membrane	Thickness (μm)		Estimated dried biovolume (mm^3)[a]		Roughness		Hydrophilicity	Surface zeta potential
	Run 1	Run 2	Run 1	Run 2	R_a (nm)[b]	R_q (nm)[c]	Contact angle (°)	(mV)
N0	N.A.	N.A.	N.A.	N.A.	118.3 ± 27.0	144.0 ± 36.0	78.7 ± 3.8	-44.3 ± 4.4
F1	2.99 ± 0.17	3.96 ± 0.26	15.0	19.8	79.2 ± 10.4	102.5 ± 17.5	90.2 ± 2.3	-17.3 ± 0.3
F2	8.80 ± 0.13	10.4 ± 0.48	44.0	52.2	61.7 ± 6.5	76.1 ± 7.6	95.5 ± 1.9	-19.2 ± 1.9
F3	26.9 ± 3.24	20.3 ± 0.43	134	102	51.1 ± 6.5	65.2 ± 8.6	107.4 ± 1.6	-25.8 ± 2.3

[a]Estimated dried biovolume was determined by multiplying the average thickness by the membrane surface area.
[b]R_a is the arithmetic average of the absolute values of the surface height deviations measured from the mean plane.
[c]R_q is the root mean square average for height deviation taken from the mean image data plane.

573 **FIGURE LEGENDS**

574
575 **Figure 1.** Log removal value (LRV) and abundance of ARGs attached on membranes.
576 (A) LRV reported in Run 1; (B) Copies of ARGs attached per surface area of membrane
577 in Run 1; (C) LRV reported in Run 2; (D) Copies of ARGs attached per surface area of
578 membrane in Run 2. ⬭ and ▭ indicate that the LRV could not be determined because the
579 $bla_{\text{CTX-M-15}}$ plasmid and $bla_{\text{OXA-48}}$ plasmid, respectively, were below the qPCR detection
580 limit for that sample.
581
582
583 **Figure 2.** ARB log removal value (LRV) of different membranes evaluated by qPCR.
584 (A) LRV for *E. coli* PI-*7* with plasmid encoding $bla_{\text{NDM-1}}$ in Run 1 and Run 2, (B) LRV
585 for *Klebsiella pneumoniae* L7 with plasmid encoding $bla_{\text{CTX-M-15}}$ in Run 1 and Run 2, (C)
586 LRV for *E. coli* UPEC-RIY-4 with plasmid encoding $bla_{\text{OXA-48}}$ in Run 1 and Run 2. (N0:
587 new membrane; N0-1, N0-2, N0-3 and N0-4 denote samples collected at 0 kPa. F1 and
588 F2: subcritically fouled membranes harvested at ~20 kPa and 40 kPa, respectively; F1-1,
589 F1-2, F1-3 and F1-4 denote samples collected at 5 kPa, 10 kPa, 15 kPa and 20 kPa,
590 respectively; F2-1, F2-2, F2-3 and F2-4 denote samples collected at 10 kPa, 20 kPa, 30
591 kPa and 40 kPa, respectively. F3: critically fouled membrane harvested at ~60 kPa; F3-1,
592 F3-2, F3-3 and F3-4 denote samples collected at 10 kPa, 20 kPa, 40 kPa and 60 kPa,
593 respectively. * indicates significant difference.)
594
595
596
597 **Figure 3.** Abundance of ARB attached per unit surface area of membrane in (A) Run 1,
598 and (B) Run 2. Abundances were quantified by qPCR. Each type of ARB attached on F1,
599 F2, and F3 was significantly higher than that attached on new membrane ($p < 0.05$).
600
601
602 **Figure 4.** Isothermal titration calorimeter (ITC) results for diluted suspension containing
603 the foulant layer of F1, F2 and F3 membranes with each ARB. The heat change for the
604 foulant layer sampled from F1, F2 and F3 and each ARB was significantly higher than
605 that measured for the control (blank).
606
607
608
609
610
611
612
613
614
615
616
617

REFERENCES

1. Rizzo, L.; Manaia, C.; Merlin, C.; Schwartz, T.; Dagot, C.; Ploy, M.; Michael, I.; Fatta-Kassinos, D., Urban wastewater treatment plants as hotspots for antibiotic resistant bacteria and genes spread into the environment: a review. *Science of the total environment* **2013,** *447*, 345-360.
2. Pruden, A.; Pei, R.; Storteboom, H.; Carlson, K. H., Antibiotic resistance genes as emerging contaminants: studies in northern Colorado. *Environmental Science & Technology* **2006,** *40*, (23), 7445-7450.
3. Mantilla-Calderon, D.; Jumat, M. R.; Wang, T.; Ganesan, P.; Al-Jassim, N.; Hong, P.-Y., Isolation and characterization of NDM-positive Escherichia coli from municipal wastewater in Jeddah, Saudi Arabia. *Antimicrobial agents and chemotherapy* **2016,** *60*, (9), 5223-5231.
4. Wen, Q.; Tutuka, C.; Keegan, A.; Jin, B., Fate of pathogenic microorganisms and indicators in secondary activated sludge wastewater treatment plants. *Journal of environmental management* **2009,** *90*, (3), 1442-1447.
5. Xu, J.; Xu, Y.; Wang, H.; Guo, C.; Qiu, H.; He, Y.; Zhang, Y.; Li, X.; Meng, W., Occurrence of antibiotics and antibiotic resistance genes in a sewage treatment plant and its effluent-receiving river. *Chemosphere* **2015,** *119*, 1379-1385.
6. Hirani, Z. M.; DeCarolis, J. F.; Adham, S. S.; Jacangelo, J. G., Peak flux performance and microbial removal by selected membrane bioreactor systems. *Water research* **2010,** *44*, (8), 2431-2440.
7. Ottoson, J.; Hansen, A.; Bjorlenius, B.; Norder, H.; Stenstrom, T., Removal of viruses, parasitic protozoa and microbial indicators in conventional and membrane processes in a wastewater pilot plant. *Water Research* **2006,** *40*, (7), 1449-1457.
8. Munir, M.; Wong, K.; Xagoraraki, I., Release of antibiotic resistant bacteria and genes in the effluent and biosolids of five wastewater utilities in Michigan. *Water research* **2011,** *45*, (2), 681-693.
9. Liao, B.-Q.; Kraemer, J. T.; Bagley, D. M., Anaerobic membrane bioreactors: applications and research directions. *Critical Reviews in Environmental Science and Technology* **2006,** *36*, (6), 489-530.
10. Xu, P.; Drewes, J. E.; Kim, T.-U.; Bellona, C.; Amy, G., Effect of membrane fouling on transport of organic contaminants in NF/RO membrane applications. *Journal of Membrane Science* **2006,** *279*, (1), 165-175.
11. Lim, A.; Bai, R., Membrane fouling and cleaning in microfiltration of activated sludge wastewater. *Journal of membrane science* **2003,** *216*, (1), 279-290.
12. van den Akker, B.; Trinh, T.; Coleman, H. M.; Stuetz, R. M.; Le-Clech, P.; Khan, S. J., Validation of a full-scale membrane bioreactor and the impact of membrane cleaning on the removal of microbial indicators. *Bioresource technology* **2014,** *155*, 432-437.

13. Cho, J.; Amy, G.; Pellegrino, J., Membrane filtration of natural organic matter: factors and mechanisms affecting rejection and flux decline with charged ultrafiltration (UF) membrane. *Journal of Membrane Science* **2000,** *164*, (1), 89-110.
14. Kiso, Y.; Nishimura, Y.; Kitao, T.; Nishimura, K., Rejection properties of non-phenylic pesticides with nanofiltration membranes. *Journal of Membrane Science* **2000,** *171*, (2), 229-237.
15. Wang, F.; Tarabara, V. V., Pore blocking mechanisms during early stages of membrane fouling by colloids. *Journal of colloid and interface science* **2008,** *328*, (2), 464-469.
16. Xiong, Y.; Harb, M.; Hong, P.-Y., Characterization of biofoulants illustrates different membrane fouling mechanisms for aerobic and anaerobic membrane bioreactors. *Separation and Purification Technology* **2016,** *157*, 192-202.
17. Yun, M.-A.; Yeon, K.-M.; Park, J.-S.; Lee, C.-H.; Chun, J.; Lim, D. J., Characterization of biofilm structure and its effect on membrane permeability in MBR for dye wastewater treatment. *Water research* **2006,** *40*, (1), 45-52.
18. Sutisna, B.; Polymeropoulos, G.; Mygiakis, E.; Musteata, V.; Peinemann, K.-V.; Smilgies, D.-M.; Hadjichristidis, N.; Nunes, S. P., Artificial membranes with selective nanochannels for protein transport. *Polymer Chemistry* **2016,** *7*, (40), 6189-6201.
19. Cheng, H.; Xie, Y.; Villalobos, L. F.; Song, L.; Peinemann, K.-V.; Nunes, S.; Hong, P.-Y., Antibiofilm effect enhanced by modification of 1, 2, 3-triazole and palladium nanoparticles on polysulfone membranes. *Scientific reports* **2016,** *6*.
20. Mantilla-Calderon, D.; Hong, P.-Y., Fate and persistence of a pathogenic NDM-1-positive Escherichia coli strain in anaerobic and aerobic sludge microcosms. *Applied and Environmental Microbiology* **2017**, AEM. 00640-17.
21. Toh, B. E.; Bokhari, O.; Kutbi, A.; Haroon, M. F.; Mantilla Calderon, D.; Zowawi, H.; Hong, P.-Y., Varying occurrence of extended-spectrum beta-lactamase bacteria among three produce types. *Journal of Food Safety* **2017**.
22. Al-Jassim, N.; Ansari, M. I.; Harb, M.; Hong, P.-Y., Removal of bacterial contaminants and antibiotic resistance genes by conventional wastewater treatment processes in Saudi Arabia: Is the treated wastewater safe to reuse for agricultural irrigation? *Water research* **2015,** *73*, 277-290.
23. Timraz, K.; Xiong, Y.; Al Qarni, H.; Hong, P.-Y., Removal of bacterial cells, antibiotic resistance genes and integrase genes by on-site hospital wastewater treatment plants: surveillance of treated hospital effluent quality. *Environmental Science: Water Research & Technology* **2017**.
24. WHO Antimicrobial resistance: global report on surveillance 2014. http://www.who.int/drugresistance/documents/surveillancereport/en/
25. Hong, P.-Y.; Al-Jassim, N.; Ansari, M. I.; Mackie, R. I., Environmental and public health implications of water reuse: antibiotics, antibiotic resistant bacteria, and antibiotic resistance genes. *Antibiotics* **2013,** *2*, (3), 367-399.
26. Wei, C.-H.; Hoppe-Jones, C.; Amy, G.; Leiknes, T., Organic micro-pollutants' removal via anaerobic membrane bioreactor with ultrafiltration and nanofiltration. *Journal of Water Reuse and Desalination* **2016,** *6*, (3), 362-370.
27. Harb, M.; Hong, P.-Y., Molecular-based detection of potentially pathogenic bacteria in membrane bioreactor (MBR) systems treating municipal wastewater: a

707 case study. *Environmental science and pollution research international* **2017,** *24*, (6),
708 5370.
709 28. Wong, K.; Xagoraraki, I.; Wallace, J.; Bickert, W.; Srinivasan, S.; Rose, J. B.,
710 Removal of viruses and indicators by anaerobic membrane bioreactor treating
711 animal waste. *Journal of environmental quality* **2009,** *38*, (4), 1694-1699.
712 29. Thomas, J. J.; Falk, B.; Fenselau, C.; Jackman, J.; Ezzell, J., Viral characterization
713 by direct analysis of capsid proteins. *Analytical chemistry* **1998,** *70*, (18), 3863-
714 3867.
715 30. Westhof, E., Water: an integral part of nucleic acid structure. *Annual review of*
716 *biophysics and biophysical chemistry* **1988,** *17*, (1), 125-144.
717 31. Faghihnejad, A.; Zeng, H., Interaction mechanism between hydrophobic and
718 hydrophilic surfaces: Using polystyrene and mica as a model system. *Langmuir*
719 **2013,** *29*, (40), 12443-12451.
720 32. Pasmore, M.; Todd, P.; Smith, S.; Baker, D.; Silverstein, J.; Coons, D.; Bowman,
721 C. N., Effects of ultrafiltration membrane surface properties on Pseudomonas
722 aeruginosa biofilm initiation for the purpose of reducing biofouling. *Journal of*
723 *Membrane Science* **2001,** *194*, (1), 15-32.
724 33. Vrijenhoek, E. M.; Hong, S.; Elimelech, M., Influence of membrane surface
725 properties on initial rate of colloidal fouling of reverse osmosis and nanofiltration
726 membranes. *Journal of membrane science* **2001,** *188*, (1), 115-128.
727 34. Baker, R.; Wijmans, J.; Athayde, A.; Daniels, R.; Ly, J.; Le, M., The effect of
728 concentration polarization on the separation of volatile organic compounds from
729 water by pervaporation. *Journal of membrane science* **1997,** *137*, (1-2), 159-172.
730 35. Jin, X.; She, Q.; Ang, X.; Tang, C. Y., Removal of boron and arsenic by forward
731 osmosis membrane: influence of membrane orientation and organic fouling. *Journal*
732 *of membrane science* **2012,** *389*, 182-187.
733 36. Tang, C. Y.; Fu, Q. S.; Criddle, C. S.; Leckie, J. O., Effect of flux (transmembrane
734 pressure) and membrane properties on fouling and rejection of reverse osmosis and
735 nanofiltration membranes treating perfluorooctane sulfonate containing
736 wastewater. *Environmental science & technology* **2007,** *41*, (6), 2008-2014.
737 37. Hoek, E. M.; Elimelech, M., Cake-enhanced concentration polarization: a new
738 fouling mechanism for salt-rejecting membranes. *Environmental science &*
739 *technology* **2003,** *37*, (24), 5581-5588.
740 38. Di Martino, P.; Cafferini, N.; Joly, B.; Darfeuille-Michaud, A., Klebsiella
741 pneumoniae type 3 pili facilitate adherence and biofilm formation on abiotic
742 surfaces. *Research in microbiology* **2003,** *154*, (1), 9-16.
743 39. Rosenberg, M.; Gutnick, D.; Rosenberg, E., Adherence of bacteria to
744 hydrocarbons: a simple method for measuring cell-surface hydrophobicity. *FEMS*
745 *microbiology letters* **1980,** *9*, (1), 29-33.
746 40. Lu, R.; Mosiman, D.; Nguyen, T. H., Mechanisms of MS2 bacteriophage
747 removal by fouled ultrafiltration membrane subjected to different cleaning methods.
748 *Environmental science & technology* **2013,** *47*, (23), 13422-13429.
749 41. Razatos, A.; Ong, Y.-L.; Sharma, M. M.; Georgiou, G., Molecular determinants of
750 bacterial adhesion monitored by atomic force microscopy. *Proceedings of the*
751 *National Academy of Sciences* **1998,** *95*, (19), 11059-11064.

42. Freire, E.; Mayorga, O. L.; Straume, M., Isothermal titration calorimetry. *Analytical chemistry* **1990,** *62*, (18), 950A-959A.
43. Formosa, C.; Grare, M.; Duval, R. l. E.; Dague, E., Nanoscale effects of antibiotics on P. aeruginosa. *Nanomedicine: Nanotechnology, Biology and Medicine* **2012,** *8*, (1), 12-16.
44. Formosa, C.; Grare, M.; Jauvert, E.; Coutable, A.; Regnouf-de-Vains, J.; Mourer, M.; Duval, R.; Dague, E., Nanoscale analysis of the effects of antibiotics and CX1 on a Pseudomonas aeruginosa multidrug-resistant strain. *Scientific reports* **2012,** *2*.
45. Lebleu, N.; Roques, C.; Aimar, P.; Causserand, C., Role of the cell-wall structure in the retention of bacteria by microfiltration membranes. *Journal of Membrane Science* **2009,** *326*, (1), 178-185.
46. Ghayeni, S. S.; Beatson, P.; Fane, A.; Schneider, R., Bacterial passage through microfiltration membranes in wastewater applications. *Journal of Membrane Science* **1999,** *153*, (1), 71-82.
47. Wang, Y.; Hammes, F.; Duggelin, M.; Egli, T., Influence of size, shape, and flexibility on bacterial passage through micropore membrane filters. *Environmental science & technology* **2008,** *42*, (17), 6749-6754.
48. Helling, A.; Kubicka, A.; Schaap, I. A.; Polakovic, M.; Hansmann, B. r.; Thiess, H.; Strube, J.; Thom, V., Passage of soft pathogens through microfiltration membranes scales with transmembrane pressure. *Journal of Membrane Science* **2017,** *522*, 292-302.
49. Gaveau, A.; Coetsier, C. m.; Roques, C.; Bacchin, P.; Dague, E.; Causserand, C., Bacteria transfer by deformation through microfiltration membrane. *Journal of Membrane Science* **2017,** *523*, 446-455.
50. Gao, W.; Lin, H.; Leung, K.; Schraft, H.; Liao, B., Structure of cake layer in a submerged anaerobic membrane bioreactor. *Journal of membrane science* **2011,** *374*, (1), 110-120.
51. Xiong, J.; Fu, D.; Singh, R. P.; Ducoste, J. J., Structural characteristics and development of the cake layer in a dynamic membrane bioreactor. *Separation and Purification Technology* **2016,** *167*, 88-96.
52. Arkhangelsky, E.; Gitis, V., Effect of transmembrane pressure on rejection of viruses by ultrafiltration membranes. *Separation and Purification Technology* **2008,** *62*, (3), 619-628.
53. Marti, E.; Monclús, H.; Jofre, J.; Rodriguez-Roda, I.; Comas, J.; Balcázar, J. L., Removal of microbial indicators from municipal wastewater by a membrane bioreactor (MBR). *Bioresource technology* **2011,** *102*, (8), 5004-5009.
54. Wu, J.; Le-Clech, P.; Stuetz, R. M.; Fane, A. G.; Chen, V., Effects of relaxation and backwashing conditions on fouling in membrane bioreactor. *Journal of Membrane Science* **2008,** *324*, (1), 26-32.

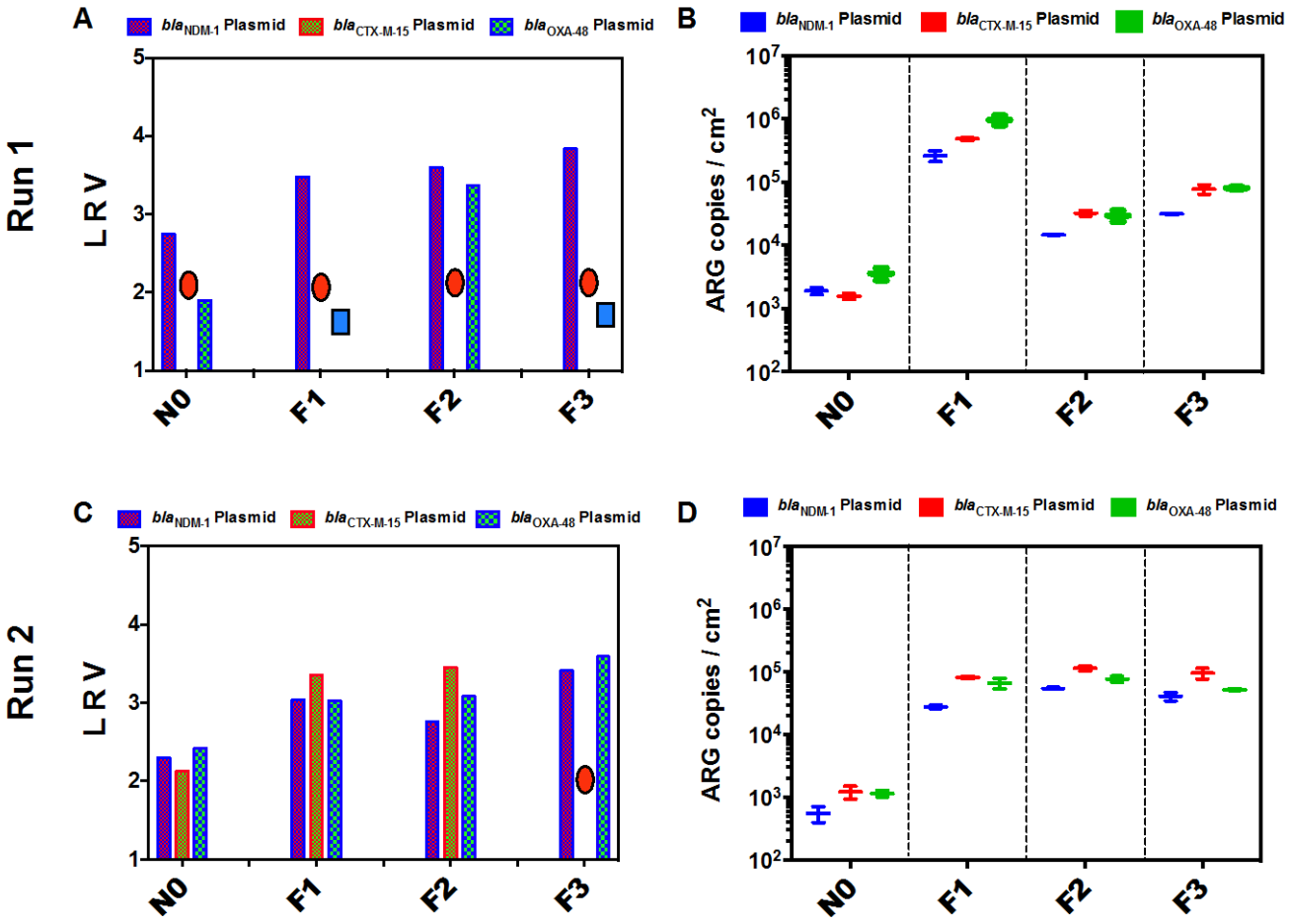
A
B
C
D
Run 1
Run 2
LRV
ARG copies / cm2
blaNDM-1 Plasmid
blaCTX-M-15 Plasmid
blaOXA-48 Plasmid
N0
F1
F2
F3

Figure 1.

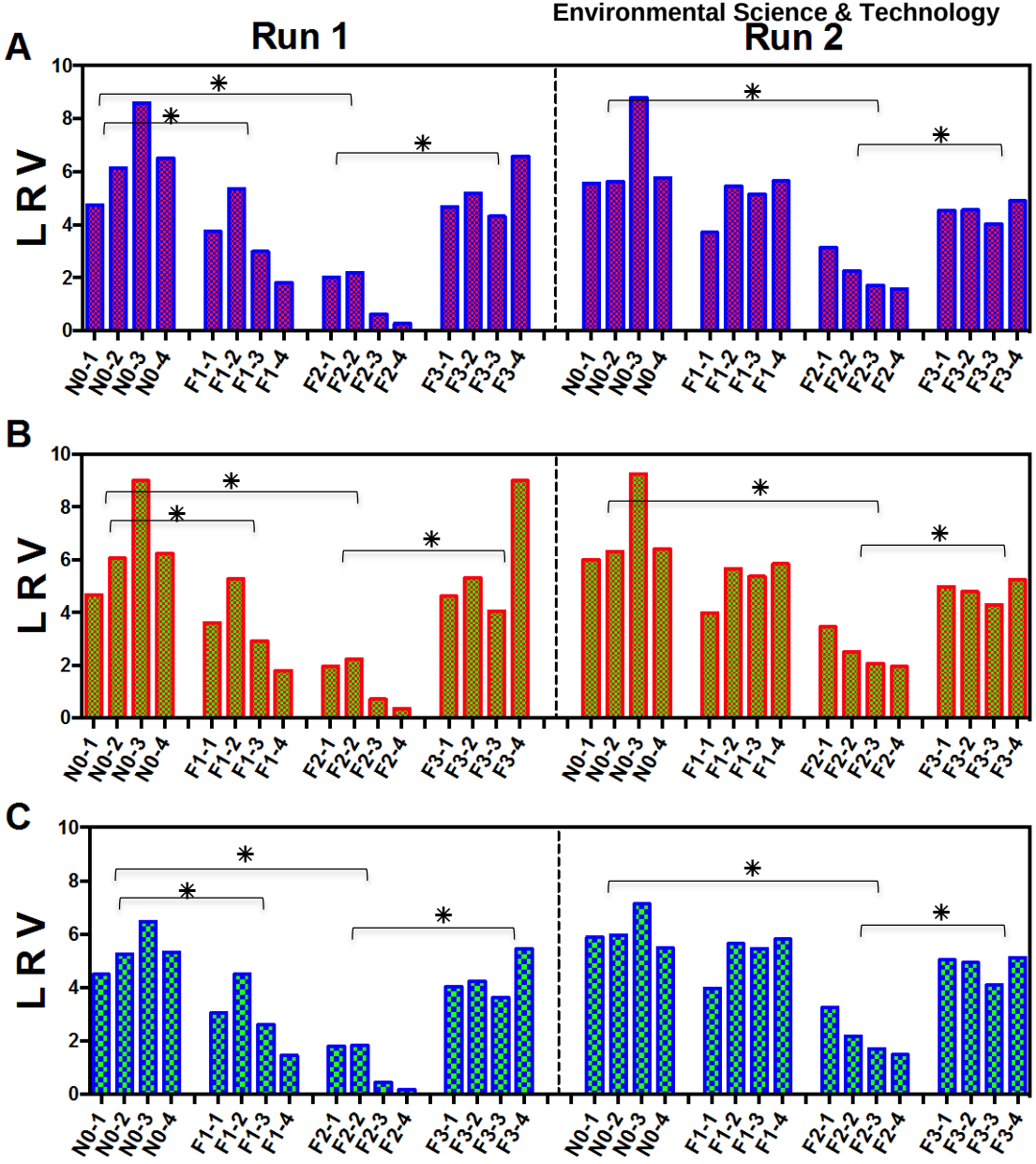

***E. coli* PI-7 with bla_{NDM-1}**

***K. pneumoniae* L7 with $bla_{CTX-M-15}$**

***E. coli* UPEC-RIY-4 with bla_{OXA-48}**

Figure 2.

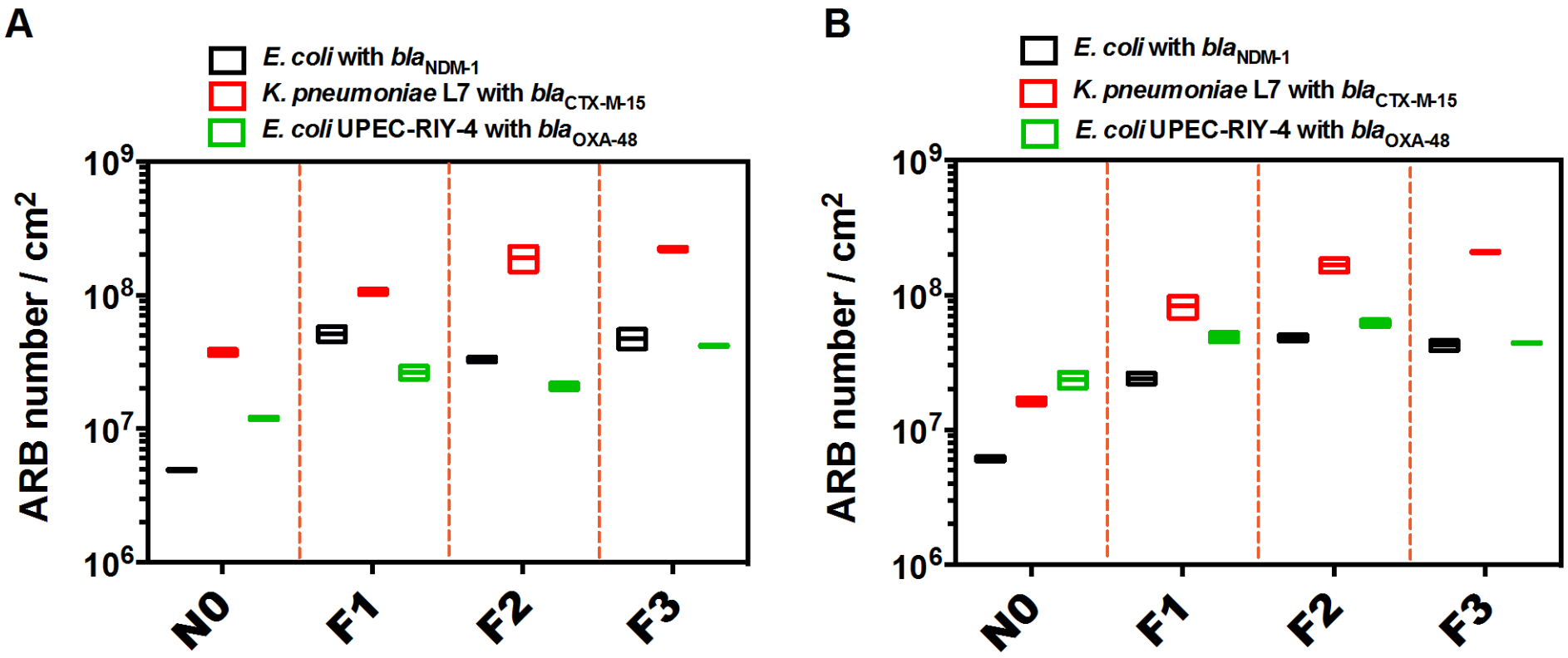
A
E. coli with bla NDM-1
K. pneumoniae L7 with bla CTX-M-15
E. coli UPEC-RIY-4 with bla OXA-48
ARB number / cm2
10^9
10^8
10^7
10^6
N0
F1
F2
F3
B
E. coli with bla NDM-1
K. pneumoniae L7 with bla CTX-M-15
E. coli UPEC-RIY-4 with bla OXA-48
ARB number / cm2
10^9
10^8
10^7
10^6
N0
F1
F2
F3

Figure 3.

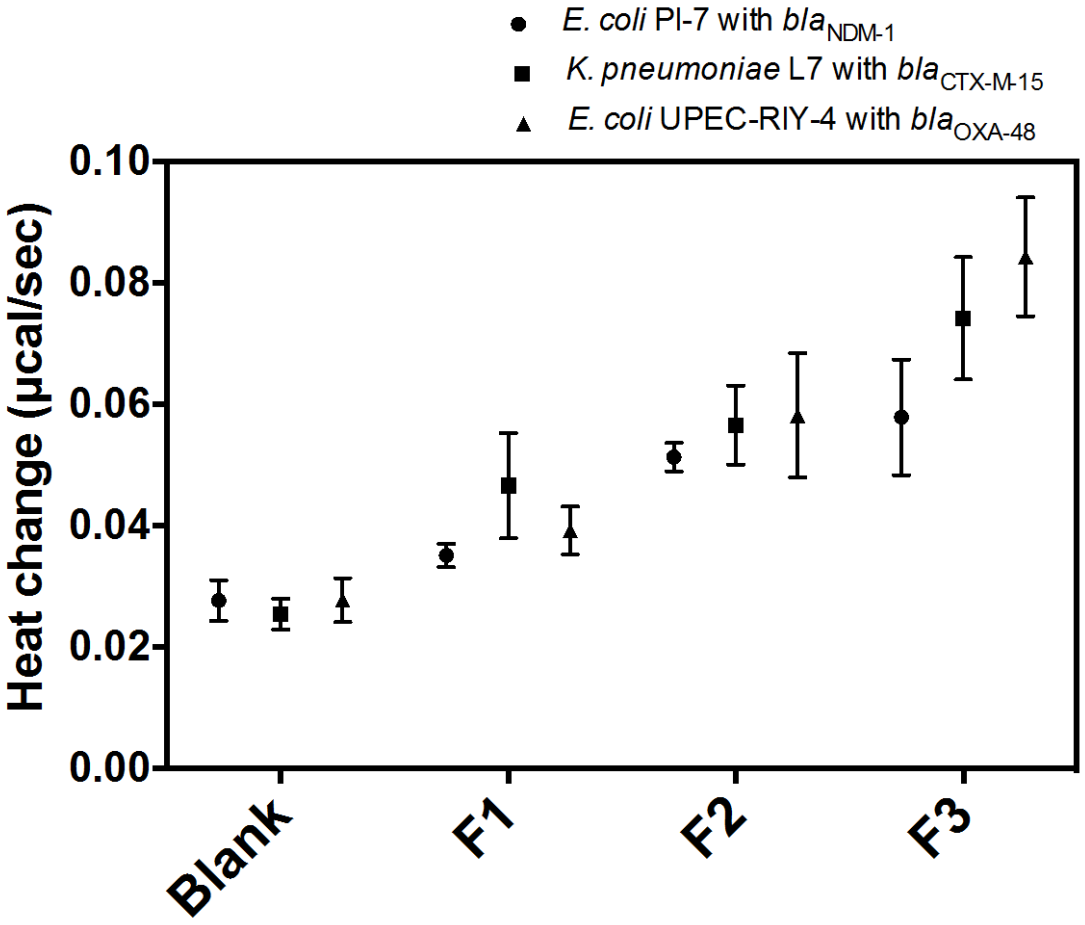
E. coli PI-7 with bla NDM-1
K. pneumoniae L7 with bla CTX-M-15
E. coli UPEC-RIY-4 with bla OXA-48
Heat change (µcal/sec)
0.10
0.08
0.06
0.04
0.02
0.00
Blank
F1
F2
F3

Figure 4.